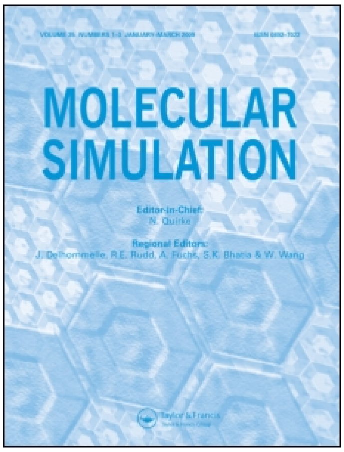

Molecular Simulation

Publication details, including instructions for authors and subscription information:
http://www.informaworld.com/smpp/title~content=t713644482

A simple model of the hydrophobic effect for molecular simulation of interfacial phenomena

Marco La Rosa[a]; Carl H. Schiesser[a]; Alfred Uhlherr[b]; Calum J. Drummond[bc]; Keith Moody[d]; Robert Bohun[d]

[a] School of Chemistry, The University of Melbourne, Vic., Australia [b] CSIRO Molecular Science, Clayton South, Vic., Australia [c] cap-XX Pty. Ltd., Lane Cove, NSW, Australia [d] Huntsman Corporation Australia Pty. Ltd., Ascot Vale, Vic., Australia

To cite this Article La Rosa, Marco , Schiesser, Carl H. , Uhlherr, Alfred , Drummond, Calum J. , Moody, Keith and Bohun, Robert(2002) 'A simple model of the hydrophobic effect for molecular simulation of interfacial phenomena', Molecular Simulation, 28: 8, 791 — 806

To link to this Article: DOI: 10.1080/0892702021000002494

URL: http://dx.doi.org/10.1080/0892702021000002494

Molecular Simulation, 2002 Vol. 28 (8–9), pp. 791–806

Taylor & Francis
Taylor & Francis Group

A SIMPLE MODEL OF THE HYDROPHOBIC EFFECT FOR MOLECULAR SIMULATION OF INTERFACIAL PHENOMENA

MARCO LA ROSA[a], CARL H. SCHIESSER[a], ALFRED UHLHERR[b,*],
CALUM J. DRUMMOND[b,c], KEITH MOODY[d] and ROBERT BOHUN[d]

[a]*School of Chemistry, The University of Melbourne, Vic. 3010, Australia;* [b]*CSIRO Molecular Science, Bag 10, Clayton South, Vic. 3169, Australia;* [c]*cap-XX Pty. Ltd., Units 9,10 and 12 Mars Rd., Lane Cove, NSW 2066, Australia;* [d]*Huntsman Corporation Australia Pty. Ltd., Newsom St., Ascot Vale, Vic. 3032, Australia*

(Received February 2001; In final form November 2001)

A coarse-grained model for simulation of interfacial phenomena in aqueous systems has been developed. The model captures the hydrophobic effect by only considering the structure and cohesiveness of water. Monte Carlo (MC) simulations of water–oil mixtures show that low concentrations of oil are solvated with little perturbation of the hydrogen bonding network structure of the water, while high concentrations of oil are excluded altogether. Analysis of the water structure in the simulations indicates that the water molecules maintain close to four coordination in the presence of solutes and the distribution of bond angles is not markedly affected by the presence of solutes. MC simulations of an alkane oligomer in water and a poly(ethylene oxide) (PEO) oligomer in water indicate that the chains are quite flexible and also do not perturb the network structure of the water phase.

Keywords: Hydrophobic effect; Water; Poly(ethylene oxide); Monte Carlo; Simulation

INTRODUCTION

It is generally accepted that the hydrophobic effect is an important factor in determining the solubility of non-polar solutes in water [1–3]. The belief that the

---

*Corresponding author. Tel.: +61-3-9545-8107. Fax: +61-3-9545-2446. E-mail: a.uhlherr@molsci.csiro.au

ISSN 0892-7022 © 2002 Taylor & Francis Ltd
DOI: 10.1080/0892702021000002494

hydrophobic effect results from the highly ordered hydrogen-bonding network and high self cohesion of water has led us to define a coarse-grained model of water which accounts for these features alone. Ultimately, we wish to simulate long-timescale interfacial phenomena, with particular emphasis on studying the phase behaviour of the nonionic surfactants of the poly(ethylene oxide) (PEO) family. However, before the model can be defined, the key issue that needs to be addressed is the level of chemical detail required. For detailed information on interfacial packing and structure over short timescales (< 5 ns), atomistic simulations would generally be most suitable [4]. However, continuum simulation of long time-scale processes such as micellisation are computationally intractable when using atomistic models. In this case, coarse-grained models are often used, and, depending on the desired results of a simulation, different models have emerged [5–9].

In the model developed by Smit and coworkers [5–8,10], two types of particle are defined; "oil-like" and "water-like". Water molecules are modelled as single water-like particles, oil molecules are modelled as single oil-like particles, while surfactants are modelled as chains of oil-like particles joined to a water-like particle. Like particles attract each other, while unlike particle interactions are purely repulsive. The authors showed that phase separation does occur and that it is indeed possible to model self-assembly processes using such a simple model. However, the model does not take into account the fact that water molecules have on average four neighbours (coordination number), nor does it account for the fact that intermolecular bonding in water (H-bonding) is much stronger than intermolecular bonding in oil (dispersion forces).

This paper presents a simple model in which chemical moieties are represented as hard spheres. Two basic types of particle are defined (water-like and oil-like) and water, oil and surfactant molecules are constructed from these particle types. Nonbonded water-like particle interactions are attractive, while all other nonbonded interactions are purely repulsive. Water-like particles have a defined maximum coordination. In this paper, we report the results of several Monte Carlo (MC) simulations including water at low density and liquid density, water–oil mixtures, an alkane oligomer in water and a PEO oligomer in water. These simulations have been chosen to test the basic physical behaviour of the model.

MODEL AND COMPUTATIONAL DETAILS

It is thought that phase separation and micellisation occur as a result of processes (the hydrophobic effect) which spontaneously remove non-polar solutes or portions of solutes from water [2]. Solvation of a non-polar solute results in the ordering of the hydrogen bond network near the solute so as to produce enough space to accommodate it. The network, however, remains essentially intact because water has a high energy of self cohesion [1]. The net result is a large decrease in entropy. Therefore, above a limiting concentration of solute in water, exclusion is favoured over solvation. Destructuring of the water molecules (near a solute) that occurs upon solute removal results in a large and positive entropy (zero enthalpy and negative free energy) [2]. For this reason we have chosen to develop a model of water which explicitly accounts for the highly ordered bonding network in water and large energy of self-cohesion in an attempt to model this behaviour.

In this model two classes of particles are defined; "water-like" and "oil-like". The atomistic analogue of an oil-like particle is one ethylene group ($CH_2{-}CH_2$). Note that in the atomistic analogues, chain ends (oil and surfactant) are terminated by $CH_2{-}CH_3$. Due to the small size of a hydrogen atom, this difference was not considered significant enough to warrant the inclusion of an extra particle type and so the term ethylene groups applies to $CH_2{-}CH_2$ pairs and $CH_2{-}CH_3$ pairs if the particle is the terminal one in an oil-like chain. These two particle types (water-like and oil-like) are used to model three types of molecules. Water molecules consist of one water-like particle, while oil molecules consist of chains of oil-like particles. We have chosen to use decane as the oil phase, therefore, oil molecules are chains of five particles. As we are interested in modelling ethylene oxide (ethoxylate) based surfactants, we have chosen to define a surfactant molecule as a chain of water-like and oil-like particles (the hydrophile) joined to a chain of oil-like particles (the hydrophobe). This model is thus more detailed than previous [5,6,10] coarse-grained surfactant models because each ethoxylate unit consists of one particle representing the oxygen and one particle representing the ethylene group. In this way, ethoxylate oxygen particles are denoted water-like and have a defined maximum total coordination.

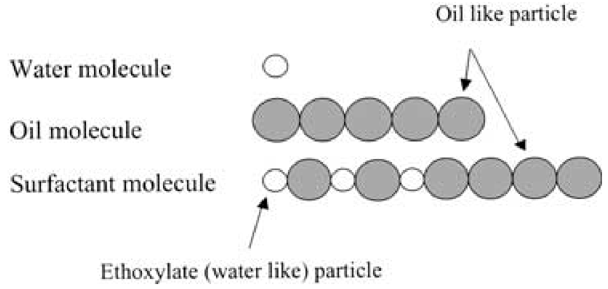

FIGURE 1 Schematic representation of the molecule types defined in this model. Light particles are water-like and dark particles are oil-like.

Consequently, the mapping to real nonionic surfactants is more direct (than other models) and the model is simplified by allowing us to define the same bonding range (hydrogen bond length) for all water-like particle interactions. A schematic representation of the molecules is shown in Fig. 1.

The particles are hard spheres which interact via variants of the square well potential. Nonbonded attractive interactions are only defined between water-like particles; a development of the "saturated square well potential" used by Speedy in his work on fluids with valency [11,12]. All other nonbonded interactions are purely repulsive. Discontinuous potentials have been chosen because of the ease with which coordination can be incorporated into the model. Up to a defined maximum coordination, nonbonded water-like particles interact via a simple square well potential. Once maximum coordination is achieved, the form of the potential changes to a purely repulsive interaction. The form of this interaction is shown in Eqs. (1) and (2).

$$U(r_{ij}) = \begin{cases} \infty & r_{ij} \leq \sigma_{ij} \\ W_{ij} & \sigma_{ij} < r_{ij} \leq \lambda_{ij}\sigma_{ij} \\ 0 & r_{ij} > \lambda_{ij}\sigma_{ij} \end{cases} \tag{1}$$

$$W_{ij} = \begin{cases} \infty & \text{if } i \text{ has } n_i \text{ neighbours or } j \text{ has } n_j \text{ neighbours} \\ +3\varepsilon & \text{if } i \text{ and } j \text{ are bonded to a common neighbour and the separation} \\ & \text{between } i \text{ and } j < \lambda\sigma \\ -\varepsilon & \text{otherwise} \end{cases} \tag{2}$$

In these equations σ_{ij} is the effective minimum separation, $\lambda_{ij}\sigma_{ij}$ is the maximum interaction distance, the energy is denoted by W_{ij} and r_{ij} is the separation between two particles i and j. The maximum total coordination of particles i and j is denoted by n_i and n_j, respectively.

If two particles i and j are close enough to interact, then if either of them has reached maximum coordination, an infinitely large energy barrier prevents the two from bonding. If neither particle has achieved maximum coordination but they are close enough to interact as well as being bonded to a common neighbour, then a penalty of 3ε is imposed and the energy of the "triangle" is zero. Otherwise, the two particles interact with an energy of $-\varepsilon$. Put more simply, two water-like particles hydrogen bonded to each other will incur an energy penalty if bonded to a common neighbour. Without this condition, water molecules tend to form clusters containing n_i particles, with each particle having exactly n_i neighbours. Once formed, these clusters remain together for the duration of the simulation with no exchange occurring, because each particle has achieved minimum energy.

Bonded interactions in chain molecules (oil and surfactant) are described in terms of an "infinite" square-well potential. That is, the energy of the bonded pair is zero when the separation is within the minimum and maximum bounds, and infinitely large if the two particles try to separate or overlap. The form of this interaction is shown in Eq. (3).

$$U(r_{ij}) = \begin{cases} \infty & r_{ij} \leq \sigma_{ij} \\ 0 & \sigma_{ij} < r_{ij} \leq \lambda_{ij}\sigma_{ij} \\ \infty & r_{ij} > \lambda_{ij}\sigma_{ij} \end{cases} \tag{3}$$

Table I lists the minimum and maximum separations of particle pairs. These values were obtained by geometric consideration of the separations of the atomistic analogues. Particles representing ethoxylate oxygens have been divided into two groups; those in the headgroup which do not have any bonded hydrogens (headgroup ether oxygens) and the terminal alcoholic oxygen which has one bonded hydrogen (hydroxyl oxygens). Table II lists the maximum total coordination (n_i) of the water-like particles and the type of particle to which they can bond. The number of bonds each can have is dependent on the number of hydrogen bonds in which the atomistic analogue can participate. For example, ether oxygens can hydrogen bond with two water particles or two hydroxyl oxygen particles (or a combination of both), but not with other ether oxygens, which have no hydrogens available for bonding.

A summary of the simulations used to validate this model is presented in Table III. The simulations were performed in the canonical ensemble (constant composition—N particles, constant volume and constant temperature) and periodic boundary conditions were imposed in all three directions. Each simulation consisted of an equilibration period of at least 1.5×10^6 cycles (1 cycle = N attempted MC moves) followed by a further 1.5×10^6 production

TABLE I Bonded and non-bonded particle pair separations for different particle types

	σ_{ij} (Å)	$\lambda_{ij}\sigma_{ij}$ (Å)
Nonbonded interactions		
Water–water, water–ethoxylate	2.50	3.20
Water–oil, ethoxylate–oil	3.17	
Oil–oil	4.00	
Bonded interactions		
Oil–oil	2.25	2.85
Oil–ethoxylate	1.75	2.15

TABLE II Types of "water-like" particles defined and the maximum total coordination (n_i) per water-like particle. The last two columns list the allowed neighbour types per water particle and the number of each allowed

Particle type	n_i	*Neighbour type*	*Maximum neighbour count*
A Water	4	A	4
		B	3
		C	2
B Hydroxyl oxygen	3	A	3
		B	2
		C	1
C Ether oxygen	2	A	2
		B	1

cycles during which data was collected. The algorithm employs a standard Metropolis MC acceptance scheme [13,14]. That is, a particle is selected randomly and displaced by a small amount in a random direction and the energy of the new configuration is evaluated. If the new configuration is lower in energy than the old configuration, the move is accepted outright; otherwise, it is accepted with a probability $p = \min[1, \exp(-\beta\Delta E)]$ where $\beta = (1/kT)$, k is Boltzmann's constant, T is the temperature and ΔE is the change in energy upon going from the old state to the new state. To speed up the calculation of the energy, a neighbour list was included and updated after every successful MC move. All of the simulations reported here were run on 600 MHz Digital DS-10 Alpha Servers.

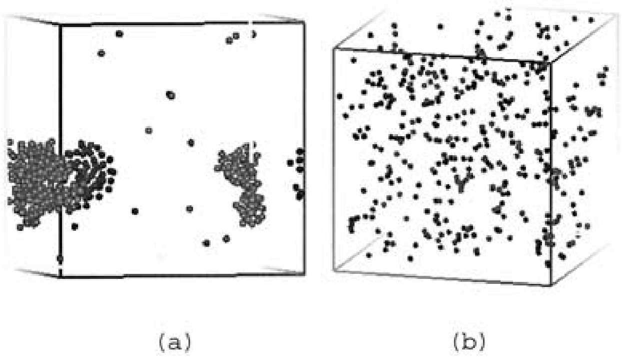

FIGURE 2 Snapshots of water at low density (i.e. fixed number of molecules in a large volume). The density of the system is 0.023 g cm^{-3}. (a) snapshot taken at the end of the simulation at 300 K (low temperature—simulation (A)), (b) snapshot taken at the end of the simulation at 450 K (high temperature—simulation (B)).

TABLE III Summary of the simulations reported in this paper. N is the total number of particles and the cell dimensions x, y, and z are calculated using the experimental densities

Label	*Simulation description*	T (K)	*Composition*	N	x (Å)	y (Å)	z (Å)
A	Low density water	300	400 water	400	80.00	80.00	80.00
B	Low density water	450	400 water	400	80.00	80.00	80.00
C	Liquid water	300	400 water	400	22.89	22.89	22.89
D	Water/oil mixed 1	300	400 water 5 decane	425	23.89	23.89	23.89
E	Water/oil mixed 2	300	400 water 25 decane	525	27.21	27.21	27.21
F	Water/oil unmixed	300	800 water 80 decane	1200	30.00	30.00	56.00
G	Long alkane in water	300	4000 water 1 × 30 unit alkane chain	4030	49.37	49.37	49.37
H	PEO in water	300	4000 water 1 × 30 unit PEO chain	4061	49.41	49.41	49.41

RESULTS

At 300 K, water at low density (low concentration of water molecules in a fixed volume) is expected to reach an equilibrium between water in the liquid and water in the vapour. Above the boiling point, the equilibrium is obviously expected to favour formation of a vapour phase. Therefore, simulation of a few water molecules in a large box (water vapour) should provide a suitable test of the cohesiveness of the model. Two simulations of water vapour were run. Both of the simulations commenced from the same initial configuration, which was generated by randomly dispersing the water molecules throughout the simulation box. The density of the system is $0.023\,\mathrm{g\,cm^{-3}}$. Figure 2(a) is the final configuration of the vapour simulation at 300 K (low temperature) while Fig. 2(b) is the final configuration of the vapour simulation at 450 K (high temperature). Quite clearly, the water molecules in the low temperature simulation have coalesced and an equilibrium has been established between water molecules in the vapour and coalesced water. Analysis of the trajectory of the low temperature simulation indicates that there is constant exchange occurring between coalesced water and water constituting the vapour phase. In contrast to this, the water molecules in the high temperature simulation have remained dispersed throughout the box. In this model, we have assumed that the strength of

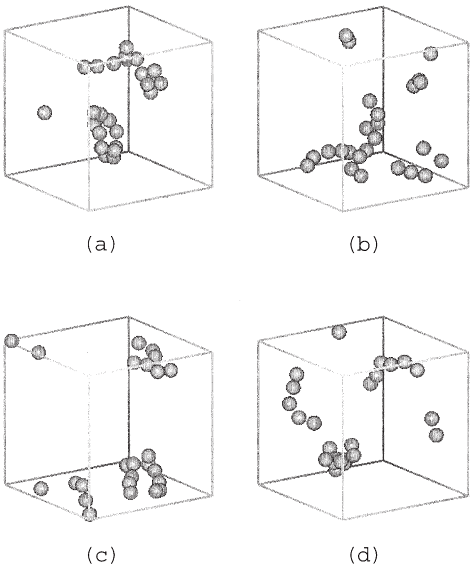
(a) (b) (c) (d)

FIGURE 3 Configurations of 5 oil molecules in bulk water (simulation D). The snapshots were taken after (a) 200,000, (b) 600,000, (c) 1,000,000 and (d) 1,500,000 production cycles.

dispersion interactions is negligible in comparison to hydrogen bonds. Therefore, the simulation boiling point of water is not expected to be quantitatively comparable to the real boiling point of water.

To examine the mixing behaviour of oil and water, three simulations of varying quantities of oil and water were run. A series of snapshots taken during the simulation of a system containing 400 water particles and 25 oil particles (simulation D) are presented in Fig. 3. The initial configuration for this system was generated by randomly dispersing oil molecules throughout the water phase. Clearly, the oil molecules are not separating out from the water molecules. Figure 4 presents a series of snapshots taken from a mixed water–oil simulation containing 400 water particles and 125 oil particles (simulation E). The initial configuration for this simulation was also generated by randomly dispersing oil molecules throughout the water phase. However, by the end of the simulation, the oil molecules can be seen to be aggregating. Analysis of the trajectories of simulations D and E show the clusters constantly breaking up and reforming, as is expected for such low concentrations of oil in water. Note that only one cluster of oil molecules is present in Fig. 4(b) and (c). The apparent semblance of two clusters is due to the location of the periodic boundaries.

In Fig. 5, two snapshots taken from a simulation of a phase separated water–oil system (simulation F) are presented. The composition of this system is 800 water

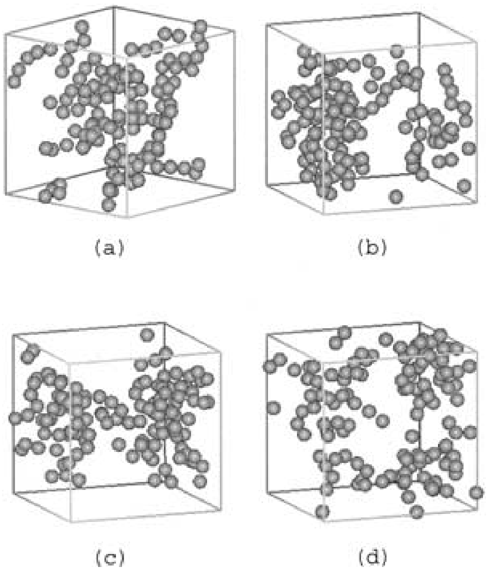

FIGURE 4 Configurations of 25 oil molecules in bulk water (simulation E). The snapshots were taken after (a) 200,000, (b) 600,000, (c) 1,000,000 and (d) 1,500,000 production cycles.

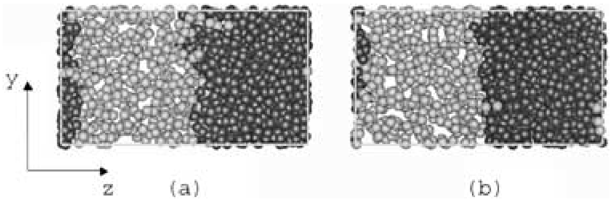

FIGURE 5 (a) the initial configuration of an unmixed water/oil simulation (simulation F) and (b) the final configuration. Light beads denote oil particles while dark beads denote water particles. The interfacial plane is perpendicular to the z direction.

particles and 400 oil particles. The initial configuration for this simulation was generated by joining together pre-equilibrated bulk water and oil phases (Fig. 5(a)). The goal of this simulation was to see whether mixing occurs in a system, which commenced in a phase-separated form. Although there is some interpenetration at the interface (Fig. 5(b)), the two phases remain distinct. The particle number density profile (Fig. 6) in the direction normal to the interface confirms this observation. From these figures it is evident that as the concentration of oil in water is increased, phase separation occurs (or in the case of simulation F, mixing does not occur), despite the absence of an explicit attractive force between the oil molecules.

To assess the behaviour of chain molecules, simulations of an alkane oligomer in water and a PEO oligomer in water were run. Snapshots taken from the alkane in water simulation are presented in Fig. 7 while snapshots taken from the simulation of a PEO chain in water are presented in Fig. 8. The alkane is a 30 unit chain corresponding to a C_{60} alkane. The PEO chain is a 61 unit chain corresponding to a 30 ethoxylate PEO chain which is terminated by hydroxyl

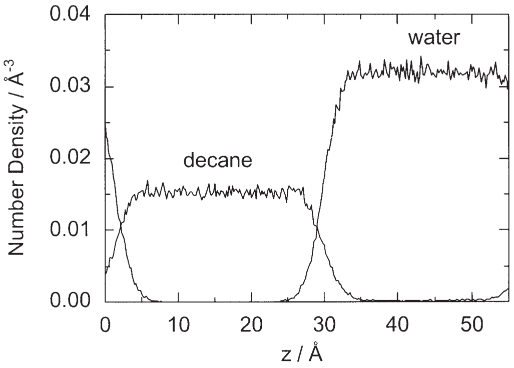

FIGURE 6 Number density profile (normal to the interface) calculated for the water–oil simulation which commenced from the phase separated initial configuration (Fig. 5—simulation F).

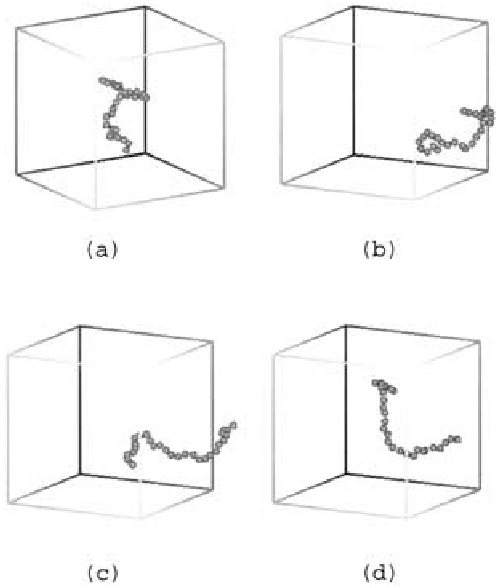

FIGURE 7 Configurations of an alkane oligomer in water (simulation G). The snapshots were taken after (a) 200,000, (b) 600,000, (c) 1,000,000 and (d) 1,500,000 production cycles.

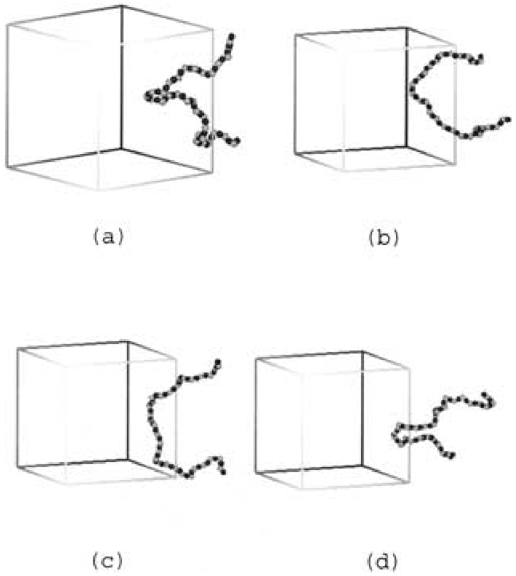

FIGURE 8 Configurations of a poly(ethylene oxide) oligomer in water (simulation H). Light beads denote the ethylene particles (oil-like) and dark beads denote the ethoxylate particles (water-like). Note that the oil-like and water-like particles are not the same size as is implied in these snapshots. The snapshots were taken after (a) 200,000, (b) 600,000, (c) 1,000,000 and (d) 1,500,000 production cycles.

oxygens at both ends. These chains were chosen so that the behaviour of the hydrophile (PEO oligomer) and the hydrophobe (alkane oligomer) could be studied independently.

From the figures it is evident that both chains are undergoing conformational changes ranging from almost fully extended to compactly coiled. Analysis of the end-to-end length distribution and radius of gyration distribution indicated that the chains have not fully sampled the accessible configuration space over the timescale of these simulations. A possible improvement of the algorithm would be to include more complex MC moves usually implemented in polymer simulation codes [15].

As a measure of the flexibility of the chains, the angle between the vectors joining a central particle to its bonded neighbours was calculated. Figure 9 shows the angular distribution calculated between ethylene–oxygen–ethylene triplets and oxygen–ethylene–oxygen triplets along the PEO oligomer. Clearly, water-like ethoxylate particles bonded to ethylene particles have a greater range of movement about the ethylene particle than ethylene particles have around ethoxylate particles. This is expected as the effective radius of the ethoxylate particles is much less than the separation of two ethylene particles. Figure 10 shows the angular distribution calculated for triplets of ethylene particles along the alkane oligomer. The greater range of movement of ethylene neighbours in the alkane oligomer as compared to the PEO oligomer is due to the larger central atom to which the neighbours are bonded (large ethylene particle compared to small ethoxylate particle).

The snapshots presented so far have addressed pictorially the behaviour of oil and oligomeric species, without any consideration to the hydrogen bonding network in the water phase in each simulation. The average coordination numbers

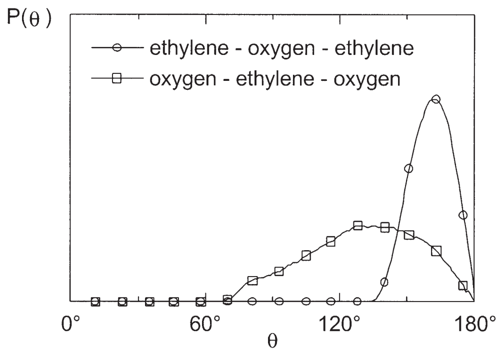

FIGURE 9 Angular distribution of ethylene–oxygen–ethylene triplets and oxygen–ethylene–oxygen triplets along the PEO chain.

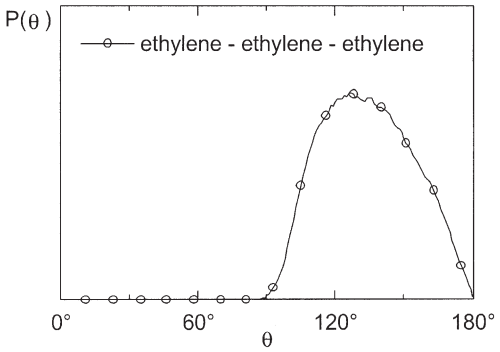

FIGURE 10 Angular distribution of ethylene–ethylene–ethylene triplets along the alkane chain.

of the water molecules in each simulation are presented in Table IV. Irrespective of the system composition, the number of neighbours per water molecule remains approximately constant. If we consider simulation D where the oil molecules remain dispersed throughout the water phase for the duration of the simulation, if the two liquids were completely miscible, it would be expected that the coordination of the water would decrease to approximately 3.64. The value of 3.81 indicates that water largely maintains its neighbour network in the presence of solutes. The same is true in simulations G and H, where the coordination number of the water particles remains close to its preferred maximum. The slightly lower values for simulations E and F are due to the presence of water–oil interfacial regions in the simulation cell. In the PEO chain, the average coordination is 2.95 for hydroxyl oxygens and 1.94 for ether oxygens. This indicates that ethoxylate particles also try to maintain maximum coordination.

The water hydrogen bond angle distribution is a useful probe of the geometry of the water network. Figure 11 shows the angular distribution curves calculated for simulations C, D, E, F, G and H. The curves are very similar, indicating that the water phase is not perturbed by the presence of solutes; irrespective of the type of solute. The calculated mean of each of the distributions is 106°. These

TABLE IV Time averaged coordination number (CN) per water molecule for each simulation

Label	*Simulation description*	*CN*
C	Liquid water	3.87
D	Water/oil mixed 1	3.81
E	Water/oil mixed 2	3.73
F	Water/oil unmixed	3.79
G	Long alkane in water	3.86
H	PEO in water	3.87

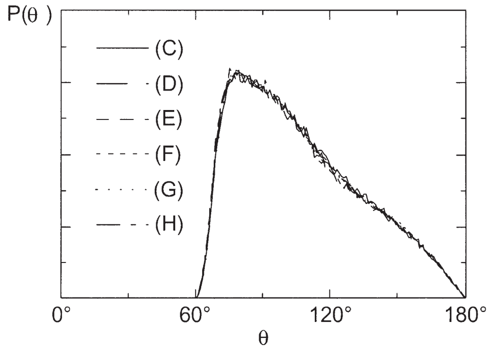

FIGURE 11 Hydrogen bond angle distributions ($P(\theta)$) for the simulations of pure water (C), water and 5 decane molecules (D), water and 25 decane (E), phase separated water–oil (F), alkane oligomer in water (G) and poly(ethylene oxide) oligomer in water (H).

distributions have been calculated using all of the water particles. Analysis of the distribution using only the water molecules in the first solvation shell of the solutes is in progress.

CONCLUSIONS

From the simulations it is evident that water modelled in this way is cohesive and maintains its structure about solvated non-polar solutes (at low concentration). However, above a limiting concentration, non-polar solutes are excluded. This compares well with the behaviour of real water, which is highly cohesive and can solubilize (without surfactant) low concentrations of oil.

Simulations of water at low density (a few molecules in a large box) showed that coalescence occurs at low temperature (300 K) while at high temperature (450 K), the molecules remain dispersed throughout the box. The observed behaviour is consistent with that of real water at low and high temperature. Simulations of mixtures of water with varying concentrations of oil showed that phase separation occurs, despite the lack of an explicit attractive interaction between the oil molecules. For low concentrations of oil in water, a dynamic equilibrium is established between solubilized oil and excluded oil. As the concentration of oil in water is increased, complete exclusion of oil is seen. Water molecules maintain close to maximum coordination and the angular distribution of water molecules is not affected by solutes. Simulations of an alkane oligomer in water and a PEO oligomer in water showed that the oligomers also do not affect the angular structure of the water phase. The local structure of the chains themselves was probed by analysis of the distribution of bonded neighbours about a central particle. The distributions indicate that the chains are highly flexible.

We are currently simulating mixtures of water, oil and nonionic (ethoxylate based) surfactants in an effort to gauge the suitability of this model for studying phase separation of mixed systems. In addition, the simulations of the alkane and PEO chain in water are being run for longer so as to accurately assess the conformational behaviour of these oligomers.

Acknowledgements

The authors gratefully acknowledge the support of an ARC SPIRT grant, No. C29805036, as well as the Melbourne Advanced Research Computing Centre (MARCC) at the University of Melbourne for the time provided on their workstation cluster. The authors would also like to thank D. Rapaport for many stimulating discussions.

References

[1] Kronberg, B., Costas, M. and Silveston, R. (1995) "Thermodynamics of the hydrophobic effect in surfactant solutions—micellization and adsorption", *Pure Appl. Chem.* **67**, 897.
[2] Paulaitis, M.E., Garde, S. and Ashbaugh, H.S. (1996) "The hydrophobic effect", *Curr. Opin. Colloid Interface Sci.* **1**, 376.
[3] Paulaitis, M.E. (1997) "Molecular thermodynamics of hydrophobic effects", *Curr. Opin. Colloid Interface Sci.* **2**, 315.
[4] Shelley, J.C. and Shelley, M.Y. (2000) "Computer simulation of surfactant solutions", *Curr. Opin. Colloid Interface Sci.* **5**, 101.
[5] Smit, B. (1988) "Molecular dynamics simulations of amphiphilic molecules at a liquid–liquid interface", *Phys. Rev. A* **37**, 3431.
[6] Smit, B., Schlijper, A.G., Rupert, L.A.M. and van Os, N.M. (1990) "Effects of chain length of surfactants on the interfacial tension: molecular dynamics simulations and experiments", *J. Phys. Chem.* **94**, 6933.
[7] Smit, B., Hilbers, P.A.J., Esselink, K., Rupert, L.A.M., van Os, N.M. and Schlijper, A.G. (1990) "Computer simulations of a water/oil interface in the presence of micelles", *Nature* **348**, 624.
[8] Smit, B., Hilbers, P.A.J., Esselink, K., Rupert, L.A.M., van Os, N.M. and Schlijper, A.G. (1991) "Structure of a water/oil interface in the presence of micelles: a computer simulation study", *J. Phys. Chem.* **95**, 6361.
[9] Palmer, B.J. and Liu, J. (1996) "Simulations of micelle self-assembly in surfactant solutions", *Langmuir* **12**, 746.
[10] Karaborni, S., van Os, N.M., Esselink, K. and Hilbers, P.A.J. (1993) "Molecular dynamics simulations of oil solubilization in surfactant solutions", *Langmuir* **9**, 1175.
[11] Speedy, R.J. (1993) "Models for fluids and crystals of molecules with valency", *J. Phys. Chem.* **97**, 2723.
[12] Speedy, R.J. and Debenedetti, P.G. (1995) "Persistence time for bonds in a tetravalent fluid", *Mol. Phys.* **86**, 1375.

[13] Metropolis, N., Rosenbluth, A.W., Rosenbluth, M.N., Teller, A.H. and Teller, E. (1953) "Equation of state calculations by fast computing machines", *J. Chem. Phys.* **21**, 1087.

[14] Allen, M.P. and Tildesley, D.J. (1987) *Computer Simulation of Liquids* (Oxford University Press, New York), pp 118–123.

[15] Leontidis, E., Forrest, B.M., Widmann, A.H. and Suter, U.W. (1995) "Monte Carlo algorithms for the atomistic simulation of condensed polymer phases", *J. Chem. Soc. Faraday Trans.* **91**, 2355.